

# Effect of Laser Illumination on Actin Polymerization and Assembly. Simultaneous Measurements Using Static and Dynamic Laser Light Scattering, Fluorescence, and Viscometry

Joyce A. Peetermans,<sup>\*,†,§</sup> Paul A. Janmey,<sup>‡</sup> Izumi Nishio,<sup>†,||</sup>  
Ken S. Zaner,<sup>‡,⊥</sup> and Toyochi Tanaka<sup>†</sup>

Department of Physics and Center for Material Science and Engineering,  
Massachusetts Institute of Technology, Cambridge, Massachusetts 02139, and  
Hematology-Oncology Unit, Massachusetts General Hospital, Department of Medicine,  
Harvard Medical School, Boston, Massachusetts 02114

Received July 20, 1989; Revised Manuscript Received May 7, 1990

**ABSTRACT:** The time course of assembly of monomeric actin (G-actin) into filaments (F-actin) was monitored by simultaneous measurement of scattered light intensity,  $I$ , effective translational diffusion coefficient,  $D$ , and fluorescence of pyrene-labeled actin. The fluorescence increases monotonically with actin polymerization. In contrast, the parameters derived from light scattering show a complex time dependence and give evidence of influence of laser illumination on actin polymerization. Extrapolation to zero laser power allowed the determination of the polymerization kinetics in the absence of laser-actin interactions. In the presence of moderate laser illumination, the scattered light intensity,  $I$ , rises more rapidly and to larger values. Simultaneously, the diffusion coefficient,  $D$ , drops more rapidly and to smaller values than at extremely low illuminating laser powers. After reaching a maximum, the scattered intensity, under nonnegligible laser illumination, drops below its plateau value for a nonilluminated F-actin sample. The size of the overshoot in  $I$  and the undershoot in  $D$  is a strong function of laser intensity. The extrema occur at approximately the time when the elongating actin filaments form a semidilute solution in which the translation of filaments is impeded. The laser-induced phenomena are eliminated by addition of very low concentrations of gelsolin, a protein that shortens the actin filaments and thus prevents the formation of an entangled semidilute phase. It is believed that the effects of laser illumination are not unique to actin networks but rather can be found in most networks of biological and synthetic polymers and can therefore have consequences for a variety of optical methods used to study the polymerization of macromolecules.

## Introduction

Laser light is commonly used in the study of the kinetics of polymerizing systems. Such studies may measure the scattered light intensity, the time autocorrelations of scattered intensity fluctuations, or the recovery of fluorescence after photobleaching. In scattering experiments, it is assumed that the laser light is elastically or quasi-elastically scattered off the sample and that the sample is not affected by the illuminating laser beam. On the other hand, interactions between laser and tissue have long been recognized and are commonly used in specialized surgical interventions. The mechanisms of interaction and the microscopic effects of the laser on the illuminated tissue have, however, not been extensively studied. In applications of laser-tissue interactions, the laser power is usually very high in a small region and the tissue is being locally burned. This can be due to global heating of the illuminated region and thus of the targeted molecules. It can also be due to absorption of the laser light by the targeted molecules only, making the laser-tissue interaction more specific. In this report, we worked with laser power levels well below the ones commonly used for medical interventions. The effect of laser radiation on the actin polymer system was, however, large. The reported experiments clearly demonstrate that laser light should be used with caution in medical applications and in the study of polymerizing synthetic and biological molecules.

Actin networks reorganize themselves slowly under weak laser illumination for a long time after most of the actin has been incorporated into the actin filaments. It is clear that the characteristics of a biopolymeric system in general can undergo serious qualitative changes in a slow equilibration process. Laser illumination, even at low powers, can contribute to such slow changes. Similar slow processes are known in synthetic gels<sup>1</sup> and could explain changes found by other investigators in long-term experiments.<sup>2,3</sup>

## Materials and Methods

**Proteins.** Actin was prepared from rabbit skeletal muscle and labeled with *N*-(1-pyrenyl)iodoacetamide as described elsewhere.<sup>4,5</sup> The fluorescence intensity of pyrene-labeled actin undergoes a 25-fold increase<sup>6</sup> when actin polymerizes. The rate of this increase has been shown to be an accurate measure of the conversion of G- to F-actin and is sensitive only to the mass of the polymer and not to the average polymer length.<sup>4,6</sup> Other assays<sup>7,8</sup> have judged pyrene-actin fluorescence not to be perfectly correlated with actin assembly. However, the deviations are primarily due to two factors, incomplete fluorescence enhancement of subunits at the end of the filament and possibly hydrolysis of ATP bound to an interior subunit.<sup>9</sup> These two effects are small in our experiments, because the number of filament ends is very small compared to the bulk actin concentration, and the polymerization is sufficiently slow for ATP hydrolysis not to lag far behind the actin polymerization. Under these conditions, the enhancement of pyrene fluorescence is a good measure of conversion of G- to F-actin.<sup>10</sup>

Pyrene-labeled G-actin was dissolved in 2 mM tris(hydroxymethyl)aminomethane (Tris), 0.2 mM ATP, 0.2 mM CaCl<sub>2</sub>, and 0.2 mM 2-mercaptoethanol, pH 7.8 (buffer A), and further purified by gel filtration on sephadex G-150 to remove traces of oligomers and other contaminants from the preparation. The reported experiments were performed on actin at a concentration of 0.20 mg/mL (Figure 1), 0.26 mg/mL (Figure 2), and 0.21 mg/mL (Figure 3). Polymerization was induced by addition of 150 mM

<sup>†</sup> Massachusetts Institute of Technology.

<sup>‡</sup> Harvard Medical School.

<sup>§</sup> Present address: Oculon, 26 Landsdowne Street, Cambridge, MA 02139.

<sup>||</sup> Present address: Department of Physics and Engineering, Aoyama-gaku University, Setagayaku T157, Tokyo.

<sup>⊥</sup> Present address: Hematology-Oncology Section, Boston City Hospital, Boston University School of Medicine, Boston, MA 02118.

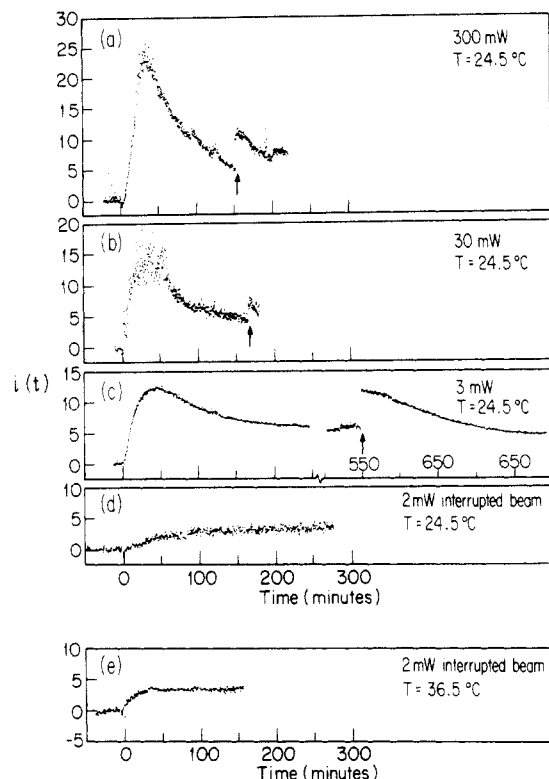


**Figure 1.** Normalized scattered intensity,  $i(t)$ , at time  $t$  relative to the onset of G-actin polymerization. In a-c the illuminating beam was, respectively, a 300-, 30-, and 3-mW argon ion laser. In d and e the laser beam was not focused, thus decreasing the power density of illumination about 13 times with respect to case c. In d and e, the beam was interrupted by a shutter for most of the time. Experiment e was performed at  $36.5^\circ\text{C}$ . Actin concentration was 0.20 mg/mL.

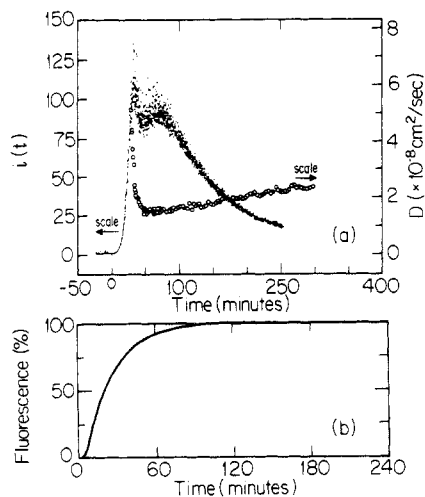


**Figure 2.** Top:  $i(t)$  represented by dots and  $D(t)$  represented by open circles, measured as a function of time in a 0.26 mg/mL polymerizing actin sample. Bottom: Fluorescence emitted by the polymerized, F-actin on the same sample, expressed in percentage polymerized material (0% for all G-actin, 100% for all F-actin).

KCl and 2 mM  $\text{MgCl}_2$ .

Gelsolin was prepared from human blood plasma by monoclonal anti-gelsolin antibody affinity chromatography by the method of Chaponnier et al.<sup>10</sup> It was used in the experiment presented in Figure 3 at an actin-gelsolin ratio of approximately 200:1, meaning that the average F-actin filament in this sample contains 200 actin monomers corresponding to a length of 450 nm.<sup>4,11</sup>

**Fluorescence.** The fluorescence intensity of the pyrene-labeled actin was measured with a Perkin-Elmer LS-5 instrument

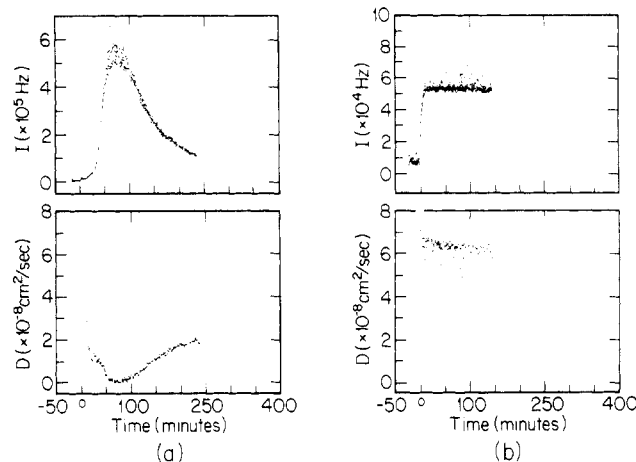


**Figure 3.** Total scattered intensity,  $I(t)$ , and diffusion coefficient,  $D(t)$ , as a function of time after onset of polymerization in a 0.21 mg/mL actin sample in the absence (a) and presence (b) of gelsolin. Illuminating laser beam was comparable to the one in Figure 1b.

using excitation and emission wavelengths of 365 and 386 nm, respectively, and a slit width of 3 nm.

**Rolling Ball Viscometry.** In order to determine if the laser illumination was capable of extensive damage to the actin network, F-actin was formed in a glass microcapillary and its viscosity measured by the rolling ball method.<sup>12</sup> Identically prepared samples were irradiated over a length of 4 cm with a succession of pulses at 577 nm, each pulse 400  $\mu\text{s}$  in duration and 36 J/cm<sup>2</sup> in intensity. The viscosity was measured by the rolling ball method immediately after completion of the irradiation.

**Static Laser Light Scattering.** The average intensity,  $I$ , of laser light scattered at an angle  $\phi$  corresponding to a wavenumber  $k$  by a solution of negligibly thin rod-shaped macromolecules can in general be expressed as

$$I(k, L, \Omega) = NM^2 f(P(kL \cos \Omega), F(k, L, \Omega))$$

where  $N$  is the number density and  $M$  the molecular weight of the macromolecules in suspension. The wavenumber is given by  $k = (4\pi/\lambda) \sin(\phi/2)$ , where  $\lambda$  is the wavelength of light in the solvent.  $1/k$  is the characteristic length scale of sample inhomogeneities that scatter light in the direction  $\phi$ , where the detector is positioned. The reported experiments were performed at  $\phi = 90^\circ$  and  $1/k = 44$  nm. The angle  $\Omega$  is the angle between the wavevector  $k$  and the direction of the rod-shaped macromolecules.  $P(kL \cos \Omega)$  is the form factor of the individual scatterers and reflects the angular dissymmetry in the scattered light intensity, which results from the finite size  $L$  of the scatterers relative to the wavenumber of the experiment.  $F(k, L, \Omega)$  is the structure factor of the solution and results from the interference between the light scattered by different individual scatterers.  $P(kL \cos \Omega)$  is normalized to 1 for a particle with characteristic length  $L$  much smaller than  $1/k$ .  $P(kL \cos \Omega)$  is smaller than 1 and oscillates as a function of  $kL \cos \Omega$  due to intraparticle interference when  $kL \cos \Omega$  is much larger than 1. On randomly oriented and strongly polydisperse samples, the form factor is a weighed average over all orientations of the  $P(kL \cos \Omega)$  for a distribution of macromolecular lengths  $L$  with average value  $\langle L \rangle$ . In such samples, composed of rod-shaped polymers with a broad length distribution in an isotropic suspension, as is the case for a suspension of F-actin filaments, the total form factor no longer shows peaks and is only a weak, monotonically decreasing function of  $k\langle L \rangle$ . In dilute, disordered samples,  $F(k, L, \Omega)$  is 1. If the scatterers form, however, a structure with characteristic lengths comparable to  $1/k$ ,  $F(k, L, \Omega)$  will in general be different from 1 and have a complicated dependence on  $k$ .<sup>13,14</sup> The dependence of  $F(k, L, \Omega)$  on  $L$  becomes increasingly weak as the typical distance between crosspoints of polymers becomes much smaller than  $L$ . For negligibly thin, isotropically oriented, polydisperse, rod-shaped macromolecules,  $f(P(kL \cos \Omega), F(k, L, \Omega))$  reduces to a simple product,<sup>13</sup> namely  $f(P(kL \cos \Omega), F(k, L, \Omega)) = P(k\langle L \rangle) F(k, \langle L \rangle)$ .

In a polymerization experiment, on the one hand, the scattered intensity increases with time as the average macromolecular

weight  $M$  increases. On the other hand, if the polymerization involves the formation of long rodlike molecules, such as is the case for F-actin formation, the growth rate of the rods will govern the rate at which  $P(kL \cos \Omega)$  decreases in time. Yet, random filament orientation and polydispersity in the long actin filament samples makes  $P(kL \cos \Omega) = P(k\langle L \rangle)$ , a smooth and slowly varying function of extent of polymerization. When the filaments form entangled networks,  $F(k, \langle L \rangle)$  becomes more significant and in fact can appreciably lower the scattered intensity,  $I$ , compared to the dilute, nonentangled system. In entangled polymers forming a regular network or homogeneous gel, the scattered intensity can become very low and relatively  $k$  independent within the typical  $k$  range of a light-scattering experiment.<sup>15</sup>

**Dynamic Laser Light Scattering.** Information about the motion of the macromolecular solute, actin monomers and polymers in this case, is extracted through an analysis of the temporal fluctuations in the scattered light intensity. The rate of the intensity fluctuations can be directly related to the rate of motion of the scatterers in the sample. For this purpose, intensity autocorrelation functions  $c(\tau)$  given by

$$c(\tau) = \langle I(t)I(t + \tau) \rangle$$

where  $\langle \rangle$  represents a time average, are formed. In the simple case of small scatterers undergoing Brownian motion,  $c(\tau)$  can be expressed as

$$c(\tau) = A \exp(-2Dk^2\tau) + B$$

where  $A$  and  $B$  are, respectively, the amplitude and base line of the correlation functions. Details of this analysis can be found elsewhere.<sup>13,16</sup> With knowledge of the wavenumber  $k$ , intensity autocorrelation spectroscopy yields the average translational diffusion coefficient,  $D$ , of the scatterers. In an entangled system of F-actin filaments,  $D$  no longer reflects free diffusion but rather should be interpreted as the collective diffusion coefficient, i.e., the ratio of the bulk osmotic incompressibility of the suspension of polymers over the friction coefficient exerted on the polymer network by the solvent.<sup>17</sup>

**Temperature.** With the exception of one experiment, all reported experiments were performed at room temperature. The static laser light-scattering experiment reported in Figure 1e was done at 36.5 °C.

## Results

Changes of total scattered intensity before, during, and after actin polymerization are shown in Figure 1. All scattered light intensity data  $I(t)$  are normalized to the value  $I_G$  corresponding to the G-actin sample prior to the onset of polymerization:

$$i(t) = [I(t) - I_G]/[I_G]$$

The moment of addition of salts to induce polymerization is defined as the zero time. In parts a–c of Figure 1, the power density of the focused, incident laser beam was, respectively,  $4 \times 10^3$ ,  $4 \times 10^2$ , and  $4 \times 10^1$  J/(s·cm<sup>2</sup>). In parts d and e of Figure 1, the laser beam was not focused and the power density was 0.3 J/(s·cm<sup>2</sup>). Moreover, this beam was interrupted by a shutter when no measurements were being made, which was about  $5/6$  of the time. The experiments shown in Figure 1a–d were performed at room temperature whereas the experiment of case e was done at 36.5 °C.

In order to demonstrate that nonilluminated regions of the actin sample have a different scattering power than the illuminated regions, the sample was carefully translated on the sample stage using a micrometer translater. The new scattered intensity  $i(t)$  was then compared to the value in previously illuminated regions of the same sample. The time at which the sample was translated is marked by an arrow in Figure 1a–c. The plotted values of  $i(t)$  after the arrow are measured on the previously nonilluminated part of the sample. Clearly, even the low laser power of 3 mW

(40 J/(s·cm<sup>2</sup>)) used in case c affects the scattering power of the sample in a dramatic way.

Compared to the room-temperature, low-illumination case of Figure 1d, the other four cases show a scattered intensity that rises faster after onset of the polymerization. In cases a–c,  $i(t)$  reaches a maximum and then drops steadily. After an initial increase, the scattered power of the nonilluminated regions stays constant. This was established by repeated translation of the sample in 30-min intervals starting hours after onset of polymerization. As soon as the beam hits the previously nonilluminated parts of the sample,  $i(t)$  starts to drop. In case a,  $i(t)$  in the region that was illuminated during early stages of polymerization reaches a value higher than the one in the nonilluminated sample part. There is an overshoot in  $i(t)$ . In case b, this overshoot is smaller. In case c, although  $i(t)$  shows a peak, the overshoot of  $i(t)$  above the value for the nonilluminated sample is absent. The experiments done at extremely low laser power and plotted in Figure 1d,e show a monotonic rise of  $i(t)$  to a plateau value. Comparison of cases d and e shows that an increase from room temperature to body temperature causes the initial rise of  $i(t)$  to be faster. However, the subsequent drop of  $i(t)$  remains absent.

The results of a typical experiment combining static laser light scattering, dynamic laser light scattering, and fluorescence measurements are shown in Figure 2. Identical samples of purified, 10% labeled actin at 0.26 mg/mL were monitored in time after onset of polymerization. Scattered intensity,  $i(t)$ , and collective diffusion coefficient,  $D(t)$ , are both measured at 2.7 J/(s·cm<sup>2</sup>) and plotted in Figure 2 (top). Fluorescence is plotted in Figure 2 (bottom). Coincident with the maximum in the scattered intensity,  $i(t)$ , the diffusion coefficient,  $D(t)$ , shows a shallow minimum. The fluorescence, reflecting the conversion from G-actin to F-actin, rises monotonically. At the time of the two extrema seen in the laser light-scattering experiments, 70% of the actin was polymerized into the F-actin form.

The light-scattering experiments were repeated with the same illumination as in the experiments shown in Figure 2 but with the aim to demonstrate that the special features of Figure 1a–c require an entangled network of polymers. A comparison was made between the static and the dynamic scattering signal from pure actin at 0.21 mg/mL and that from the same actin sample with a 1:200 molar ratio of gelsolin added to limit filament length. In the first sample, the actin forms a network of entangled filaments; in the second sample the actin filaments, cut by gelsolin, are too short to be entangled (see the Discussion). The resulting data are given in parts a and b of Figure 3, respectively. They show the scattered intensity,  $I(t)$ , and the effective diffusion coefficient,  $D(t)$ , for each sample. The measurements of  $D(t)$  on the G-actin sample prior to polymerization are not shown. The value is approximately  $7.5 \times 10^{-7}$  cm<sup>2</sup>/s and was reported elsewhere.<sup>18</sup> Clearly, both the overshoot and the subsequent steady drop of the scattered intensity are absent in the gelsolin-containing sample. The effective diffusion coefficient,  $D(t)$ , falls to a plateau value shortly after onset of polymerization in the sample with gelsolin. In the pure actin sample, however,  $D(t)$  shows a shallow minimum coincident with the maximum in the scattered intensity. It should be noted that the asymptotic value of  $D(t)$ , though clearly higher than its minimum value, is still very much lower than the value of  $D$  for G-actin prior to polymerization. The asymptotic value for  $I(t)$  in comparison is much lower than the value at the peak.

**Capillary viscometry** was performed on well-equilibrated F-actin samples in microcapillary tubes. Extremely slow falling ball times were recorded, confirming the formation of an entangled F-actin network. The tube was irradiated over a length of 4 cm with a succession of laser pulses at 577 nm, each pulse 400  $\mu$ s in duration and 36 J/cm<sup>2</sup> in strength. The irradiation amounted to approximately  $9 \times 10^4$  J/(s·cm<sup>2</sup>), which is a power density about 22 times higher than that in the case of Figure 1a. No change was observed in the falling ball times.

## Discussion

**General Significance of Laser-Polymer Interactions.** Although evidence of an effect of prolonged low power laser illumination on polymer and network formation was demonstrated here only for actin systems, we feel the observed phenomena might be of more general significance. The work to which we made reference earlier in this paper<sup>1-3</sup> does by no means constitute the only papers in which there seemed to be documented evidence of slow laser-polymer interactions. We are presently investigating the general nature of the phenomena reported here on actin systems by doing similar experiments on other biopolymeric systems as well as on synthetic polymer systems. In the meantime we suggest that it might be very worthwhile for investigators using prolonged low laser level illumination as a means to monitor ongoing polymerization or other slow equilibration processes to make sure that effects of laser illumination on the system under study can be ruled out. The effect of laser illumination is subtle and, at this time, only partially understood.

**Initial Enhancement of the Rate of Polymerization.** It is very likely for the initial enhancement of the rate of polymerization to be caused by a small degree of local heating in the illuminated portion of the sample. Indeed, the rate of growth of polymers is known to be a sensitive function of temperature. The experiments presented in Figure 1 d,e confirm this finding. In case d the temperature was 24.5 °C, and in case e it was 36.5 °C. The initial slope of  $i(t)$  is appreciably steeper at the higher temperature. No measurement was made of the local temperature in the small illuminated region of the sample in the higher laser power experiments of Figure 1a-c, Figure 2 (top), and Figure 3a. We consider it possible for this local temperature to reach values markedly higher than 24.5 °C. This, we believe, could cause the actin filaments to grow to lengths longer than their equilibrium length. The overshoot in  $i(t)$  could thus reflect an unstable state caused by temperature-induced enhanced polymerization.

**Drop in  $i(t)$  Requiring Entangled Polymers.** From the fluorescence data, we know the concentration of polymer at the time of maximum scattered intensity. When the actin filaments are approximated by rigid rods diffusing freely up to this point, the diffusion coefficient  $D$  measured by dynamic laser light scattering yields the average length of the polymers. A similar analysis was performed using Broersma's formula<sup>19</sup> in a previous study.<sup>18</sup> The combination of the measured polymer concentration and this average filament length reveals that the maximum scattered intensity is reached in the neighborhood of the onset of the semidilute or entangled network phase. For example, in the case of Figure 3, the diffusion coefficient at the minimum is  $1.75 \times 10^{-8}$  cm<sup>2</sup>/s, which corresponds to an average length of 1.3  $\mu$ m according to Broersma's formula for rigid rods and a filament width of 0.01  $\mu$ m. Fluorescence measurements on an identically treated sample show that the actin filament concentration at this point in time is 60% of the total 0.21 mg/mL actin

concentration, which amounts to 0.13 mg/mL. The concentration  $c^*$  above which a polymer system becomes semidilute assuming monodisperse, rigid rodlike filaments is approximately given by<sup>20</sup>

$$c^* \text{ (in mg/mL)} = (n_L/V_L)f_c = 4.88 \times 10^{-10}/L^2 \text{ (in cm}^2\text{)}$$

where  $n_L$  is the number of actin monomers in a filament of length  $L$ ,  $V_L$  is the volume occupied by a sphere of radius  $L/2$ , and  $f_c$  is the factor that converts the number of actin molecules to milligrams of actin. The values used were  $3.7 \times 10^6$  actin monomers/cm<sup>11</sup> and 24  $\mu$ M per mg/mL of actin. For 1.3- $\mu$ m filaments,  $c^*$  is 0.03 mg/mL. Though this is about 4 times smaller than the measured concentration at the time of maximum scattered intensity, it does indicate that the sample is very close to the onset of the semidilute regime. In fact, it is well-known that appreciable diffusional retardation does not occur for rodlike particles until one is well into the semidilute regime. Moreover, the actin samples are not monodisperse. Instead, they contain a wide range of filament lengths. Scattered light intensity is weighed by the square of the size of the scattering molecules. Therefore, the values for  $D$  at all times are more heavily weighted toward the longer filaments, and the above-derived average filament length  $L$  is thus longer than the number-average length of the filaments in the sample. The concentration  $c^*$  for onset of the entangled phase is thus underestimated in the above analysis. Quantifying exactly by how much  $c^*$  was underestimated requires a detailed analysis of the distribution of lengths of the filaments.

**Shortened Filament Sample.** The gelsolin-containing sample yields light-scattering results shown in Figure 3b. Clearly, they resemble the results found for very low illumination plotted in Figure 1d,e. The average filament length at the 1:200 gelsolin-actin ratio should be 0.54  $\mu$ m. The corresponding diffusion coefficient using Broersma's<sup>19</sup> formula is  $3.2 \times 10^{-8}$  cm<sup>2</sup>/s. The measured value of  $D = 6.5 \times 10^{-8}$  cm<sup>2</sup>/s is reasonably close and may reflect that the sample with gelsolin contains rather rigid, monodisperse, and dilute filaments. The onset of the semidilute phase for filaments with  $D = 6.5 \times 10^{-8}$  cm<sup>2</sup>/s is at  $c^* = 0.78$  mg/mL. When  $i(t)$  for the gelsolin-containing sample stops rising and reaches its plateau value, the fluorescence measurements show that 90% of the actin has gone into the filament form. At 90% of 0.21 mg/mL, this corresponds to 0.19 mg/mL actin concentration, less than  $c^*$  (0.78 mg/mL). Thus the actin filaments in the gelsolin-containing sample are not entangled. This, we believe, is why the laser-induced drop in  $i(t)$  is absent in this sample despite laser illumination similar to the one in Figure 1a. Moreover, the diffusion coefficient in Figure 3b stays constant after reaching the lowest value; there seems to be no filament breakage in this gelsolin-containing sample.

**Slow Drop in  $i(t)$ .** The drop of the scattered intensity observed in Figure 1 a-c, Figure 2a, and Figure 3a could, at first sight, be explained in a few different ways. There could be convective flow in the sample cell such that it would align the actin filaments in the illuminated region. There could be breakage of the long actin filaments due to laser illumination. The laser illumination could cause the F-actin to align as a result of induced polarity in the filaments. The laser beam could cause the entangled network of actin filaments to become more regular in a slow equilibration process. There could well be yet other contributions to the observed phenomena. Though we give slightly more information with regard to the four suggestions listed above, we are unable at this point to fully explain the reported observations.

A convective flow pattern around the illuminated region could preferentially drag longer filaments into this region. This would contribute to the initial relative enhancement of scattered intensity and subsequently to the progressive decrease of the structure factor  $F(k, \langle L \rangle)$ . Yet, it would also be accompanied by the occurrence and progressive increase of the depolarized scattered intensity. Measurement of the intensity of depolarized scattered light revealed only extremely small depolarization and no increase of it in time. We feel therefore that alignment due to convective flow in the sample cell is unlikely. Moreover, we observed no thermal lensing in the pattern of the laser beam transmitted through the samples.

We feel that actin filament breakage is not the cause for the slow but very significant drop of the scattered intensity  $i(t)$  upon laser illumination. This is based on the capillary viscometry experiment described above. Nevertheless, it should be pointed out that the laser irradiation to which the actin samples were exposed in the falling ball experiment originated from short, high-intensity pulses. The total amount of energy to which the F-actin samples were exposed by the pulsed laser was higher than the total amount of energy to which the F-actin samples were exposed in experiments such as the one plotted in Figure 1a. However, the rate of energy deposition is much higher in the pulsed laser experiment. We cannot rule out the possibility that this plays a role in the effect of laser illumination on actin networks. Yet, the observed drop in  $i(t)$ , if due solely to filament breakage, should be accompanied by a simultaneous rise of  $D(t)$  much larger than the observed, weak rise of  $D(t)$  after reaching a shallow minimum in experiments such as the one of Figure 1a.

The third suggestion for a contribution to the dramatic drop in  $i(t)$  with illuminated time is related to the dipole moment induced by the electromagnetic field of the laser beam in the actin filaments. The energy gain,  $U$ , associated with placing an actin filament and its induced dipole moment in the electric field of the laser beam is proportional to the filament volume. Calculation<sup>21</sup> of the maximum value of this energy for the configuration of this experiment—300-mW laser and  $50 \times 10^{-4}$ -cm beam waist radius—on a  $10^{-4}$ -cm-long filament shows that  $U$  is much smaller than  $kT$ , the thermal energy at room temperature. Thus filaments were not pulled into the laser beam during the experiment. We feel, however, that it cannot be entirely ruled out that F-actin molecules trapped in the beam due to the strong entanglement of the actin network, experience a slight bias toward alignment in the electric field of the laser. This may contribute somewhat to the slow organization of the network, which will be further addressed in the next paragraph. Experiments are presently being planned for further and systematic investigation of this point.

A suggestion that, indeed, seems consistent with all our data is that the laser beam slowly causes the actin network to become more regular. This may be the result of the above-stated polarization and/or may be the result of local heating. We estimate, using the expressions of Simon et al.,<sup>22</sup> that this heating could, after some 150 min of illumination, reach a few degrees above ambient. The exact value for this temperature rise depends on the absorbance,  $A$ , of the actin suspensions at the laser wavelength

and on the thermal conductivity,  $K$ , of the suspension. We have only estimates of  $A$  and  $K$  for our particular samples at this point, yielding temperature rises in the beam waist of at most 5 °C above ambient after 150 min. Though it is clear from the experiment performed at body temperature and presented in Figure 1e that such a temperature increase uniformly throughout the sample does not cause the observed  $i(t)$ , this issue is under closer investigation. Previous work<sup>3</sup> demonstrated that synthetic polymer gels prepared at slightly higher temperatures are optically clearer than ones prepared at lower temperatures. This is attributed to the fact that a more regular network structure on the length scale of  $1/k$  presents less inhomogeneity in the refractive index of the medium and thus makes for less light scattering. The dynamic data on the diffusion coefficient are not in contradiction with this. Indeed,  $D$  in the entangled phase is to be interpreted as the ratio of incompressibility of the actin network to the friction coefficient exerted on the actin network.  $D$  would be slightly altered in the formation of a more orderly network but not to the extent to which it would reach values that approximate values for monomeric actin. This is in agreement with our experimental findings.

**Acknowledgment.** We thank Dr. Thomas Stossel at the Massachusetts General Hospital for his help and fruitful discussions during this study. We thank Dr. Oon Tan at Boston University for kindly providing the pulsed laser required in the falling ball experiments of this study. Some of us acknowledge the NIH for support through Grants 2R01EY05272-04A1 (T.T.), AR38910 (P.A.J.), and GM37590 (K.S.Z.).

## References and Notes

- Carlson, F. D.; Fraser, A. B. *J. Mol. Biol.* **1974**, *89*, 273.
- Fujime, S.; Ishiwata, S.; Maeda, T. *Biophys. Chem.* **1984**, *20*, 1.
- Sun, S. T.; Tanaka, T. Private communications.
- Janmey, P. A.; Stossel, T. P. *J. Muscle Res. Cell Motil.* **1986**, *7*, 446.
- Kouyama, T.; Mihashi, K. *Eur. J. Biochem.* **1981**, *114*, 33.
- Cooper, J. A.; Walker, S. B.; Pollard, T. D. *J. Muscle Res. Cell Motil.* **1983**, *4*, 253.
- Grazi, E. *Biochem. Biophys. Res. Commun.* **1985**, *128*, 1058.
- Grazi, E. *Arch. Biochem. Biophys.* **1987**, *257*, 115.
- Carlier, M. F.; Pantaloni, D.; Korn, E. D. *J. Biol. Chem.* **1986**, *261*, 10785.
- Chaponnier, C.; Janmey, P. A.; Yin, H. L. *Cell Biol.* **1986**, *103*, 1473.
- Hanson, J.; Lowy, J. *J. Mol. Biol.* **1963**, *6*, 46.
- Ishimoto, C. Ph.D. Thesis, Department of Biology, Massachusetts Institute of Technology, 1978.
- Berne, B. J.; Pecora, R. *Dynamic Light Scattering with Applications to Chemistry, Biology and Physics*; John Wiley and Sons: New York, 1976.
- For example: Pusey, P. N. *Philos. Trans. R. Soc. London, A* **1979**, *293*, 429.
- Tanaka, T. *Sci. Am.* **1981**, *244*, 124.
- Chu, B. *Laser light scattering*; Academic Press: New York, 1974.
- Einstein, A. *Ann. Phys.* **1905**, *17*, 549.
- Janmey, P. A.; Peetermans, J. A.; Zaner, K.; Stossel, T. P.; Tanaka, T. *J. Biol. Chem.* **1986**, *261*, 8357.
- Broersma, S. J. *J. Chem. Phys.* **1960**, *32*, 1632.
- Janmey, P. A.; Lind, S. E.; Yin, H. L.; Stossel, T. P. *Biophys. Biochim. Acta* **1985**, *841*, 151.
- Stratton, J. A. *Electromagnetic theory*; McGraw-Hill Book Company: New York and London, 1941; pp 194–217.
- Simon, J. R.; Gough, A.; Urbanik, E.; Wang, F.; Lanni, F.; Ware, B. R.; Taylor, D. L. *Biophys. J.* **1988**, *54*, 801.